

Are your **MRI contrast agents** cost-effective?

Learn more about generic **Gadolinium-Based Contrast Agents**.



**FRESENIUS  
KABI**

caring for life

**AJNR**

## **Exophytic Lumbar Vertebral Body Mass in an Adult with Back Pain**

J.C. Benson, M.A. Vizcaino, D.K. Kim, C. Carr, P. Rose, L. Eckel and F. Diehn

*AJNR Am J Neuroradiol* published online 20 August 2020  
<http://www.ajnr.org/content/early/2020/08/20/ajnr.A6749>

This information is current as of April 17, 2024.

# Exophytic Lumbar Vertebral Body Mass in an Adult with Back Pain

J.C. Benson, M.A. Vizcaino, D.K. Kim, C. Carr, P. Rose, L. Eckel, and F. Diehn

## ABSTRACT

**SUMMARY:** Chordomas are rare primary bone malignancies derived from notochord remnants. The tumors often are slow-growing and often present with indolent, nonspecific symptoms. Nevertheless, chordomas are locally aggressive and highly prone to local recurrence, necessitating precise planning before biopsy and/or surgical resection. Familiarity with the imaging features of chordomas is, therefore, essential. This case highlights the typical imaging and pathologic features of a spinal chordoma as well as the surgical approach and the patient's subsequent outcome.

In brief, this case involves a 70-year-old man presented with a 1-month history of low-back and bilateral thigh pain that was unresponsive to physical therapy or chiropractic care. His symptoms were exacerbated by standing and walking and affected his left leg more than the right one. He had no known malignancy; his medical history was unremarkable except for atrial fibrillation. The patient had undergone MR imaging at an outside institution that had shown a mass in his lumbar spine. He subsequently presented to our institution for further care.

### Imaging

An initial lumbar spine radiograph demonstrated a destructive lesion in the L3 vertebral body with endplate deformities (not shown). Subsequent MR imaging confirmed the presence of a large left-eccentric exophytic mass arising from L3 (Fig 1). Although some internal heterogeneity was noted, the tumor was predominantly hypointense on T1WI and markedly hyperintense on T2WI. The mass demonstrated heterogeneous areas of solid and linear enhancements, some corresponding to T2-hypointense intratumoral septations. The moderately enhancing tumor extended into the adjacent soft tissues, displacing the left psoas muscle and narrowing the left L3–4 foramen, with pushing rather than infiltrative-appearing margins. CT, too, showed a large destructive mass arising from the L3 vertebral body. No intralaminar calcifications were noted within the lytic tumor. A whole-body nuclear medicine bone scan (not shown) showed neither

convincing activity nor photopenia in the corresponding region, nor were metastases seen elsewhere.

The marked T2 hyperintensity of the tumor, internal T2-hypointense septations, and large extrasosseous components were suggestive of a chordoma. Chondrosarcoma was considered, though classic “rings and arcs” were not observed. Giant cell tumors are found much more commonly in the sacrum, but they share many similar imaging characteristics with chordomas when seen in the mobile spine. Plasmacytomas typically remain within the bone and often have a “minibrain” or “soap bubble” intratumoral appearance.<sup>1</sup> Finally, a solitary metastasis, though possible, was thought unlikely given the appearance of the mass and the lack of known primary malignancy.

The likelihood of a chordoma or chondrosarcoma had implications for immediate management. A contemplated biopsy, for example, should be carefully planned and well-documented because the entire biopsy track is often resected or radiated in cases of chordoma or sarcoma to prevent local recurrence. Some surgeons even prefer the entry site of any percutaneous biopsy to be marked to facilitate the subsequent resection of the track.

### Operative Report and Follow-Up

The patient's surgical resection was performed in a staged, en bloc fashion (Fig 2). On the first day, the patient underwent an anterior, transperitoneal approach to mobilize the visceral and vascular structures away from the tumor. Additionally, because the extrasosseous tumor extended above the L2–3 and below the L3–4 disc spaces laterally and endplate fractures had allowed tumor entry into the disc spaces, osteotomies cut through the lower portion of the L2 vertebral body and the upper portion of the L4 vertebral body to allow removal of the specimen without inadvertent entry into the tumor.

Received May 4, 2020; accepted after revision June 2.

From the Departments of Radiology (J.C.B., D.K.K., C.C., L.E., F.D.), Pathology (M.A.V.), and Orthopedic Surgery (P.R.), Mayo Clinic, Rochester, Minnesota.

Please address correspondence to John C. Benson, MD, 200 1st St. SW, Department of Radiology, Mayo Clinic, Rochester, MN 55905; e-mail: [benson.john3@mayo.edu](mailto:benson.john3@mayo.edu)  
<http://dx.doi.org/10.3174/ajnr.A6749>

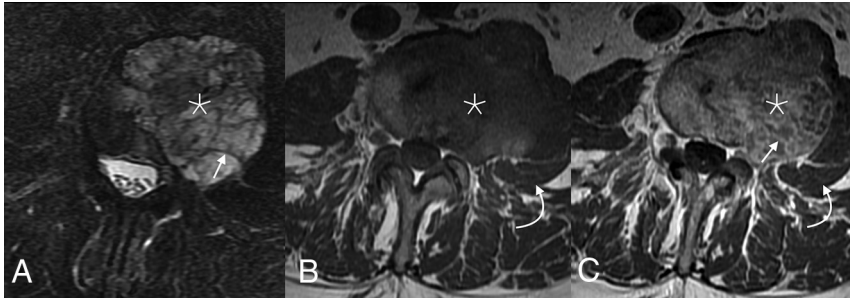


**FIG 1.** Axial MR imaging of the mass. T2 fat-saturated (A), T1 precontrast (B), and postcontrast (C) sequences show a mass centered within the mid and left aspects of the L3 vertebral body (*asterisk*). Most of the tumor demonstrates substantial T2 prolongation, which is particularly evident with fat saturation. Internal T2-hypointense septations are noted, which enhance with moderate avidity (*straight arrows*), while the fluid-filled regions lack enhancement. The tumor extends out of the left vertebral body into the adjacent soft tissues, displacing but not invading the left psoas muscle laterally (*curved arrows*).

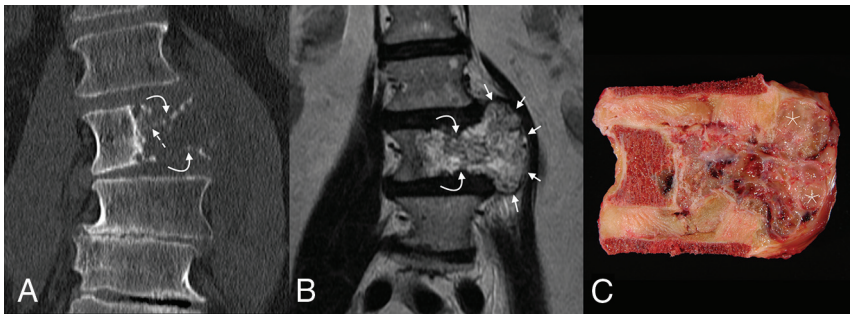


**FIG 2.** Coronal imaging and corresponding gross pathology of the tumor. On CT (A), the mass is destructive, with faint small foci of high attenuation, either representing amorphous calcifications or residual/partially destroyed vertebral body trabeculae (*dashed arrow*). Both the superior and inferior endplates are fractured (*curved arrows*). The degree of extraosseous extension is best seen on T2 MR imaging (B), where the soft-tissue components are seen to mushroom out along the adjacent intervertebral discs (*between the short arrows*), with pushing-type margins. The gross pathology specimen (C) confirms the presence of numerous high-water-content loculations (*asterisk*) separated by small septations, corresponding with areas of T2 hyperintensity.

The patient returned to surgery 48 hours later for posterior tumor delivery and an instrumented spinal reconstruction. This involved laminectomies from the lower portion of L2 through the upper portion of L4 for exposure of the dural tube, sacrifice of the bilateral L2 and L3 nerve roots, and completion of osteotomies through L2 and L4 for en bloc tumor delivery. Reconstruction was performed with a combination of posterior pedicle screw instrumentation, bone autograft, and an anterior titanium cage.

Three years after the patient's en-bloc L3 vertebrectomy with tumoral resection, he was diagnosed with a recurrent lesion in his L4 vertebral body and adjacent paraspinal soft tissues, seen on both PET and MR imaging. This was treated with cryoablation. Imaging performed during the subsequent 18 months demonstrated no other recurrences or metastases. The remainder of the patient's follow-up course was completed at an outside institution. He ultimately died 6 years postoperatively from complications related to Parkinson disease and had asymptomatic local recurrence at the time of his death.

## Pathology

Histologic sections demonstrated a neoplasm arranged in nests and cords within a prominent myxoid mucoid matrix (Fig 3). Most of the tumor cells were large, round-to-oval, with central nuclei and abundant eosinophilic cytoplasm with mild vacuolation. Scattered physaliphorous cells with multivacuolation and a foamy appearance were also present. Only rare mitoses were identified. Immunohistochemistry performed on paraffin-embedded tissue demonstrated nuclear brachyury and cytoplasmic keratin CAM 5.2 expression in the neoplastic cells (Figs 3C, -D). The tumor was also immunoreactive for vimentin, while S-100 protein was negative.

Despite chondrosarcoma in the differential diagnosis of chordoma, the lack of chondroid differentiation in this case along with the presence of physaliphorous cells favored the diagnosis of chordoma. Given the growth pattern and myxoid background of this neoplasm in addition to keratin immune expression, metastatic carcinoma was another diagnostic consideration. Nonetheless, brachyury is a highly sensitive and specific marker expressed in chordoma and negative in chondrosarcoma and carcinoma. On the basis of the morphologic and immunophenotypic findings, the diagnosis of chordoma was rendered.

## Diagnosis: Chordoma

**Discussion.** Chordomas are primary bone malignancies that typically occur in adults older than 40 years of age and affect men more than women.<sup>2,3</sup> The tumors are rare, with an incidence of 0.08 per 100,000 individuals, accounting for 1%–8% of primary bone tumors.<sup>4</sup> However, they do represent up to 20% of primary bone tumors of the spine.<sup>5</sup> The tumors arise from vestigial notochord remnants, which typically involute during the tenth week of gestation.<sup>5</sup> This embryologic origin likely explains the observed anatomic proclivity for the clivus, spine, and sacrum.<sup>6</sup> The distribution among these sites is relatively evenly split, with roughly one-third of chordomas arising from each site, though vertebral bodies are typically described as the least commonly involved.<sup>7</sup> Within the spine, however, cervical segments are most often involved, particularly C2. The pathogenesis of chordomas also explains the tumoral predilection for midline or paramedian locations because notochordal remnants evolve into the nucleus pulposus.

On imaging, chordomas usually appear as destructive osseous masses with involvement of the adjacent soft tissues.<sup>8</sup> Many tumors are large at the time of diagnosis, owing to their indolent

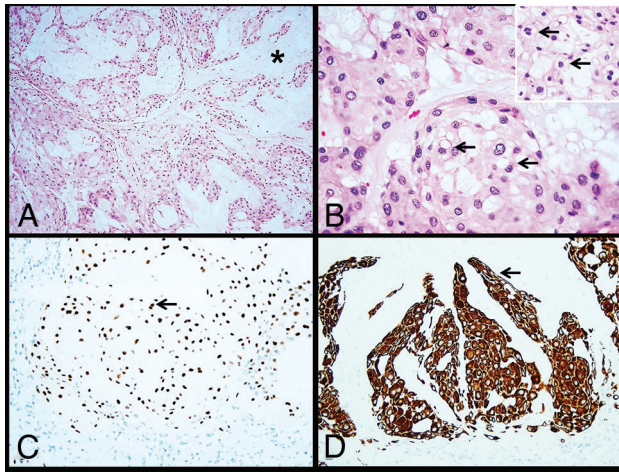


**FIG 3.** Histology images. The tumor consists of cells arranged in nests and cords (A) within an abundant mucoid matrix (A, asterisk). Most of the tumor cells are large with central nuclei and mildly vacuolated eosinophilic cytoplasm (B, arrows). Scattered physaliphorous cells are also present (B inset, arrows). Immunohistochemistry demonstrates nuclear brachyury (C, arrow) and cytoplasmic keratin CAM 5.2 (D, arrow) expression in tumor cells.

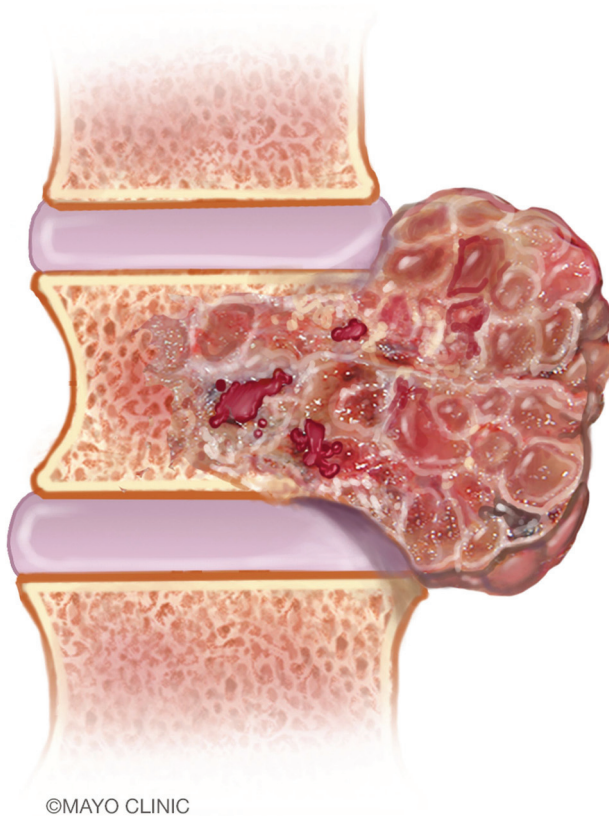


**FIG 4.** An artist's illustration of a spinal chordoma. The tumors are generally sizable at the time of diagnosis. Extrasosseous components are often larger than those within the vertebral bodies and extend along the adjacent spinal segments, compatible with the classically described dumbbell appearance. Image used with permission of Mayo Foundation for Medical Education and Research. All rights reserved.

growth. The appearance exhibited is often that of a “dumbbell” or “mushroom” configuration, in which the exophytic component is more expansile than the vertebral body from which the tumor originates.<sup>9</sup> Due to the indolent growth of the malignancy, the margins of the tumor tend to displace adjacent tissue rather than invade it. The paraspinal component can extend along the margins of  $\geq 1$  adjacent vertebral body but typically spares the intervertebral disc (Fig 4). Infrequently, tumors may spread into the paraspinal soft tissues via the neural foramina, simulating the appearance of a schwannoma.<sup>10</sup>

On CT, chordomas tend to be lobulated, osteolytic, expansile, and exophytic. Intratumoral attenuation is low due to the presence of myxoid-type tissue. Punctate calcifications and/or flecks of residual or destroyed bone are often present.<sup>11</sup> These calcifications appear amorphous and are found in higher concentrations near the tumor margins.<sup>12</sup> On MR imaging, the most notable feature is that of striking intratumoral T2 prolongation due to high internal water content. Although not pathognomonic, markedly elevated T2 signal within a lobulated midline spinal mass is highly suggestive of a chordoma. Areas of intrinsic T1 hyperintensity are often present, representing hemorrhage or mucinous material. Varying degrees of enhancement can be seen. The fibrous septa separating the T2 bright mucinous regions of the tumor tend to be T2 hypointense and enhancing.<sup>13</sup> However, a minority of chordomas may not enhance, and this subset may have a lower risk of posttreatment recurrence in a skull base location.<sup>14</sup> Finally, diffusion-weighted imaging may have diagnostic and prognostic value: Lower ADC values both favor chondroma over chondrosarcoma and predict chordoma tumor progression.<sup>15,16</sup>

The imaging findings in this case fit many of the classic descriptors of a chordoma. The tumor was large, osteolytic, exophytic, and demonstrated striking intratumoral T2 signal separated by more hypointense septations. Its dumbbell shape—owing to a large extrasosseous component that had well-defined rather than infiltrating margins that extended along the spine—was particularly distinctive. Chondrosarcomas share many of these features but typically have an intratumoral chondroid matrix (Table). Giant cell tumors lack the internal T2 hyperintensity seen in this tumor and typically occur in younger patients. Plasmacytoma was thought less likely because of the prominent intratumoral septations. A solitary metastasis, though possible, was considered lower on the differential, given the patient's lack of a primary malignancy.

Histologically, chordomas also have several characteristic features. Macroscopically, the tumors are made up of lobulated gelatinous gray tissue that may appear encapsulated. Chordomas are formed by large vacuolated cells forming nests and strands within a myxoid mucoid matrix.<sup>17</sup> Cellularity can be variable, and some tumors may show solid areas. Physaliphorous cells are round-to-oval with central nuclei and abundant cytoplasm with prominent perinuclear vacuolation. Although classic in chordomas, these cells may be sparse-to-rare in some cases. Mitotic activity is generally low. Chordomas may exhibit foci of chondroid differentiation, particularly those arising in the spheno-occipital region.<sup>18</sup> In rare cases, a spindle cell component with features of malignant fibrous histiocytoma can be noted; such tumors are designated as dedifferentiated chordomas.<sup>19</sup> Immunohistochemically, chordomas demonstrate

## Comparison of various demographic, location, and imaging features of chordomas with those of the most common imaging differential diagnoses

	Chordoma	GCT	Chondrosarcoma	Plasmacytoma
Age at diagnosis (range) (peak yr)	40–60	20–30	30–70	30–60
Most common location in mobile spine	Cervical	Lumbar (sacrum much more common)	Lumbar	Thoracic
Commonly involves posterior elements	–	+	+	+
Intratumoral calcification	Amorphous	–	Rings and arcs	–
T2WI	↑↑	↓→	↑	↑
Extraosseous extension	+	+	+	–
Characteristic feature	Dumbbell or mushroom shape	Lytic lesion without sclerotic rim; fluid-fluid levels	Intratumoral chondroid matrix	Minibrain, soap bubble

**Note:**—GCT indicates Giant cell tumor; –, features absent; +, features present; ↓→, hypo- to iso-intense intralesional signal; ↑, hyperintense intralesional signal.

nuclear positivity for brachyury, which is highly sensitive and specific for this tumor. It can also express keratin CAM 5.2, epithelial membrane antigen, vimentin, and S-100 protein.<sup>20</sup> The differential diagnosis of chordoma includes chondrosarcoma and metastatic carcinoma. Even though chondrosarcomas can mimic chordomas morphologically (especially if the latter shows extensive chondroid differentiation), chondrosarcoma is negative for brachyury by immunohistochemistry and has frequent *isocitrate dehydrogenase 1 and 2 (IDH1/IDH2)* gene mutations. In contrast, chordoma is consistently immunoreactive for brachyury and does not show *IDH1/IDH2* mutations.<sup>21</sup> Metastatic carcinomas are also immunoreactive for keratins. However, they are also positive for other organ-specific markers and do not express brachyury.

Although slow-growing, chordomas are locally aggressive malignancies, often displacing adjacent structures.<sup>22</sup> Overall, the prognosis of chordomas is poor, with a median survival of 6.3–7.7 years, and a 5-year survival rate of 68%–72%.<sup>23,24</sup> Resected tumors often recur locally and are thought to be seeded by the pseudocapsule at the tumor margins.<sup>24</sup> Thus, achieving negative margins during surgery is paramount in the treatment of such tumors. Recurrences have poor prognoses, with substantially worsened 5- and 10-year survival than primary tumors.<sup>25</sup> Radiation treatment has also been shown to improve local control and overall survival, and cryoablation and laser interstitial thermal therapies have been reported for treatment of recurrences.<sup>26–28</sup> Large tumor size, intratumoral necrosis, and advanced age are also associated with worse outcomes.<sup>10</sup> Metastases, conversely, are rare, even in the setting of large tumors. When present, metastases usually occur late in the disease course.<sup>29</sup>

### Case Summary

- Chordomas of the mobile spine classically have a mushroom or dumbbell shape and striking intratumoral T2 hyperintensity, with T2-hypointense septations.
- Diagnostic considerations include chondrosarcoma, giant cell tumor, plasmacytoma, and solitary metastasis.
- Suspicion of a chordoma should be communicated to ensure careful planning of any future biopsy and/or surgical resection.
- Brachyury immunohistochemistry is very helpful to distinguish chordoma from other mimics.

- Resection with wide surgical margins is essential to prevent local recurrences.

Disclosures: Peter Rose—UNRELATED: Consultancy: K2M, Comments: prior preliminary design contract to develop spine oncology implants: total ~\$5000, all donated to charity; Travel/Accommodations/Meeting Expenses Unrelated to Activities Listed: Depuy Spine, Comments: prior expense reimbursement while chairing a spine tumor educational course; donated to charity.

### REFERENCES

1. Major NM, Helms CA, Richardson WJ. The “mini brain”: plasmacytoma in a vertebral body on MR imaging. *AJR Am J Roentgenol* 2000;175:261–63 [CrossRef Medline](#)
2. Pendharkar AV, Ho AL, Sussman ES, et al. Surgical management of sacral chordomas: illustrative cases and current management paradigms. *Cureus* 2015;7:e301 [CrossRef Medline](#)
3. Zhou Y, Hu B, Wu Z, et al. A giant lumbar chordoma: a case report. *Medicine (Baltimore)* 2018;97:e11128 [CrossRef Medline](#)
4. Smoll NR, Gautschi OP, Radovanovic I, et al. Incidence and relative survival of chordomas: the standardized mortality ratio and the impact of chordomas on a population. *Cancer* 2013;119:2029–37 [CrossRef Medline](#)
5. Muneer M, Badran S, Al-Hetmi T. A rare presentation of axial chordoma and the approach to management. *Am J Case Rep* 2019;20:773–75 [CrossRef Medline](#)
6. Godkin O, Elkhwad H, McCabe J. Large chordoma of the sacrum. *BMJ Case Rep* 2017;2017:bcr2017221293 [CrossRef Medline](#)
7. Frezza AM, Botta L, Trama A, et al. Chordoma: update on disease, epidemiology, biology and medical therapies. *Curr Opin Oncol* 2019;31:114–20 [CrossRef Medline](#)
8. Farsad K, Kattapuram SV, Sacknoff R, et al. Sacral chordoma. *Radiographics* 2009;29:1525–30 [CrossRef Medline](#)
9. Smolders D, Wang X, Drevelengas A, et al. Value of MRI in the diagnosis of non-clival, non-sacral chordoma. *Skeletal Radiol* 2003;32:343–50 [CrossRef Medline](#)
10. Noor A, Bindal P, Ramirez M, et al. Chordoma: a case report and review of literature. *Am J Case Rep* 2020;21:e918927 [CrossRef Medline](#)
11. Murphey MD, Andrews CL, Flemming DJ, et al. From the archives of the AFIP: primary tumors of the spine—radiologic pathologic correlation. *Radiographics* 1996;16:1131–58 [CrossRef Medline](#)
12. Krol G, Sundaresan N, Deck M. Computed tomography of axial chordomas. *J Comput Assist Tomogr* 1983;7:286–89 [CrossRef Medline](#)
13. Rodallec MH, Feydy A, Larousserie F, et al. Diagnostic imaging of solitary tumors of the spine: what to do and say. *Radiographics* 2008;28:1019–41 [CrossRef Medline](#)
14. Lin E, Scognamiglio T, Zhao Y, et al. Prognostic implications of gadolinium enhancement of skull base chordomas. *AJNR Am J Neuroradiol* 2018;39:1509–14 [CrossRef Medline](#)

15. Yeom KW, Lober RM, Mobley BC, et al. **Diffusion-weighted MRI: distinction of skull base chordoma from chondrosarcoma.** *AJNR Am J Neuroradiol* 2013;34:1056–61.S1 [CrossRef Medline](#)
16. Sasaki T, Moritani T, Belay A, et al. **Role of the apparent diffusion coefficient as a predictor of tumor progression in patients with chordoma.** *AJNR Am J Neuroradiol* 2018;39:1316–21 [CrossRef Medline](#)
17. MacLean FM, Soo MY, Ng T. **Chordoma: radiological–pathological correlation.** *Australas Radiol* 2005;49:261–68 [CrossRef Medline](#)
18. Wasserman JK, Gravel D, Purgina B. **Chordoma of the head and neck: a review.** *Head Neck Pathol* 2018;12:261–68 [CrossRef Medline](#)
19. Shih AR, Cote GM, Chebib I, et al. **Clinicopathologic characteristics of poorly differentiated chordoma.** *Mod Pathol* 2018;31:1237–45 [CrossRef Medline](#)
20. Oakley GJ, Fuhrer K, Seethala RR. **Brachyury, SOX-9, and podoplanin, new markers in the skull base chordoma vs chondrosarcoma differential: a tissue microarray-based comparative analysis.** *Mod Pathol* 2008;21:1461–69 [CrossRef Medline](#)
21. Arai M, Nobusawa S, Ikota H, et al. **Frequent IDH1/2 mutations in intracranial chondrosarcoma: a possible diagnostic clue for its differentiation from chordoma.** *Brain Tumor Pathol* 2012;29:201–06 [CrossRef Medline](#)
22. Phang ZH, Saw XY, Nor N, et al. **Rare case of neglected large sacral chordoma in a young female treated by wide en bloc resection and sacrectomy.** *BMC Cancer* 2018;18:1112 [CrossRef Medline](#)
23. McMaster ML, Goldstein AM, Bromley CM, et al. **Chordoma: incidence and survival patterns in the United States, 1973–1995.** *Cancer Causes Control* 2001;12:1–11 [CrossRef Medline](#)
24. Pillai S, Govender S. **Sacral chordoma: a review of literature.** *J Orthop* 2018;15:679–84 [CrossRef Medline](#)
25. Ailon T, Torabi R, Fisher CG, et al. **Management of locally recurrent chordoma of the mobile spine and sacrum.** (*Phila Pa 1976*) 2016;41: S193–98 [CrossRef Medline](#)
26. Indelicato DJ, Rotondo RL, Begosh-Mayne D, et al. **A prospective outcomes study of proton therapy for chordomas and chondrosarcomas of the spine.** *Int J Radiat Oncol Biol Phys* 2016;95:297–303 [CrossRef Medline](#)
27. Williams BJ, Karas PJ, Rao G, et al. **Laser interstitial thermal therapy for palliative ablation of a chordoma metastasis to the spine: case report.** *J Neurosurg Spine* 2017;26:722–24 [CrossRef Medline](#)
28. Kurup AN, Woodrum DA, Morris JM, et al. **Cryoablation of recurrent sacrococcygeal tumors.** *J Vasc Interv Radiol* 2012;23:1070–75 [CrossRef Medline](#)
29. Fourny DR, Gokaslan ZL. **Current management of sacral chordoma.** *Neurosurg Focus* 2003;15:1–5 [CrossRef Medline](#)